Effects of Salmonella Typhimurium Infection on Intestinal Flora and Arachidonic Acid Metabolism in Wenchang Chickens

Shenghong Chen , Yaochen Xie , Dingqian Guo , Tiansen Li , Zhen Tan , Xuhua Ran * , Xiaobo Wen *

Posted Date: 17 April 2024

doi: 10.20944/preprints202404.1170.v1

Keywords: Salmonella Typhimurium; gut microbiota; lipid oxidation; arachidonic acid; Wenchang chicken

 doi:10.20944/preprints202404.1170.v1

Article

Effects of *Salmonella Typhimurium* Infection on Intestinal Flora and Arachidonic Acid Metabolism in Wenchang Chickens

Shenghong Chen, Yaochen Xie, Dingqian Guo, Tiansen Li, Zhen Tan, Xuhua Ran * and Xiaobo Wen *

School of Tropical Agriculture and Forestry, Hainan University, Haikou 570228, Hainan, China
* Correspondence: ranxuhu@hainanu.edu.cn (X.R.); xiaobo_wen@hainanu.edu.cn (X.W.)

Simple Summary: Wenchang chicken, as a local breed in Hainan Province, is important to the poultry farming industry. Exploring the effect of *Salmonella* infection on Wenchang chickens can provide theoretical support for developing healthy breeding and controlling the infectious disease. We examined the changes in intestinal flora and oxidized lipid metabolism in intestinal tissues of Wenchang chickens before and after *Salmonella* infection. The results showed that the cecum microbial community of Wenchang chickens significantly changed after infection with *Salmonella Typhimurium* (*S. Typhimurium*), with a significant decrease of beneficial bacterial (e.g., *Bifidobacterium*, *Lactobacillus*, and *Odoribacter*). *S. Typhimurium* infection significantly increased the levels of key enzymes for ARA production and metabolism (PLA2 and COX-2) and ARA metabolites (e.g., PGE2, PGF2α, 5-OxoETE, LXA4, and (±8(9)-EET) in the cecum tissue of Wenchang chickens. Cyclooxygenase inhibitors reduced the increased levels of COX-2 and PGF2α in HD11 cells infected by *S. Typhimurium* and effectively reduced the inflammatory response. It suggests that *S. Typhimurium* can mediate the onset and development of intestinal inflammation through activation of the chicken ARA cyclooxygenase metabolic pathway. Thus, our results provide theoretical support for the control of avian salmonellosis.

Abstract: *Salmonella* infections can lead to intestinal inflammation and metabolic disorders in birds. However, whether ARA metabolism is involved in Salmonella-induced intestinal inflammation remains unclear. This experiment investigated the changes in cecal flora and arachidonic acid (ARA) metabolism in Hainan Wenchang chickens infected with *S. Typhimurium* using 16s rDNA sequencing and targeted metabolomics. The results showed that the levels of ARA metabolites were increased in the cecum tissue of Wenchang chickens after infection with *S. Typhimurium*, including prostaglandin E2, prostaglandin F2α, lipoxin A4, ±8(9)-EET, ±11(12)-EET, and ±8,9-DiHETrE. The content of key enzymes for ARA production and metabolism (PLA2 and COX-2) in chicken cecum tissues was increased after *S. Typhimurium* infection. The relative mRNA levels of inflammatory factors were also increased after infection, including IFN-γ, TGF-β1, IL-4, and IL-6. In HD11 cells, the use of a cyclooxygenase (COX) inhibitor reduced the increased levels of COX-2 and PGF2α induced by *S. Typhimurium* infection and effectively reduced the inflammatory response. In addition, the number of beneficial genera (e.g., *Bifidobacterium*, *Lactobacillus,* and *Odorobacterium*) in the cecum of Wenchang chickens was significantly reduced after infection with *S. Typhimurium*. In this study, we revealed the structure of the cecal flora of Wenchang chickens infected with *S. Typhimurium* and demonstrated that *S. Typhimurium* can mediate the onset and development of intestinal inflammation through the activation of the metabolic pathway of ARA cyclooxygenase in Wenchang chickens. The results can provide data support and theoretical support for the prevention and control of avian salmonellosis.

Keywords: *Salmonella Typhimurium*; gut microbiota; lipid oxidation; arachidonic acid; Wenchang chicken

 doi:10.20944/preprints202404.1170.v1

1. Introduction

Salmonella is one of the most common intestinal pathogens in animals and humans. In poultry, *Salmonella enteritidis* (*S. Enteritidis*) and *Salmonella Typhimurium* (*S. Typhimurium*) infections are insidious and usually asymptomatic or cause intestinal inflammation. Moreover, *Salmonella spp.* can compete with the normal microbiota in various ways, disrupting its balance and causing a decline in the immunity of livestock and poultry, which, in severe cases, can cause high mortality [1,2]. The impact and economic loss to the poultry industry are significant by reducing meat and egg production, breeder fertility, and embryo hatchability [3].

Gut microbial communities play an important role in avian health. For example, the ability of *Campylobacter* to infect chickens is influenced by gut flora [4]. Host immune responses are strongly correlated with changes in the abundance of intestinal bacteria; for example, the expression of the pro-inflammatory cytokine interleukin 6 (IL-6) is positively correlated with *Shigella*, *Parasuttterella*, and *Vampirovibrio* and negatively correlated with *Fecalbacterium* [5]. Therefore, it is essential to have a comprehensive understanding of the effects of *Salmonella* infection on the intestinal flora of poultry, which can help control the disease's occurrence and development. Wenchang chickens are the most economically valuable indigenous livestock species in Hainan Province [6]. However, little is known about the changes in their intestinal flora after *Salmonella* infection.

The ability of *S. Typhimurium* to use the respiratory electron acceptor tetrathionate, which is produced during inflammation, provides it with a growth advantage over other flora in the inflamed gut environment [2]. Thus, controlling the development of intestinal inflammation might help enhance resistance to intestinal colonization by *Salmonella* [2]. Inflammation is regulated by inflammatory mediators, and the arachidonic acid (ARA) metabolic pathway in the polyunsaturated fatty acid metabolic network has been reported to be the major route by which inflammatory mediators are produced [7,8]. ARA and its metabolic derivatives (ARA-like) are involved in pathophysiological processes related to cell injury, inflammation, and apoptosis. For example, they are involved in physiological processes such as blood leukocyte chemotaxis, platelet aggregation, and the promotion of intestinal inflammation by mediating Th17 and Th1 cells [7,9]. It has been reported that infection of human intestinal epithelial cell lines (Caco2 and HT29) with both enteroinvasive *Escherichia coli* and *Salmonella* significantly increased cyclooxygenase two expression and prostaglandin E2 (PGE_2) production [10]. Increased prostaglandin F2α ($PGF_{2\alpha}$) release was also observed in intestinal epithelial cells following *Salmonella* infection [11]. PGE_2, 5-HETE, 8-HETE, 12-HETE, and 15-HETE syntheses were increased in Caco2 cells after lipopolysaccharide (10 g/mL) treatment [12]. However, the question of whether ARA metabolites mediate the development of avian *Salmonella* enteritis has not been reported. Therefore, given the critical role of ARA and its metabolites in mediating the inflammatory response, it is essential to elucidate the metabolic changes of ARA in intestinal tissues following *Salmonella* infection. The metabolic changes of ARA in the intestinal tissues of Wenchang chickens after *S. Typhimurium* infection were detected by ultra-high performance liquid chromatography-tandem mass spectrometry (UHPLC-MS/MS). This study further explored the potential link between ARA metabolic pathways and avian *Salmonella* enteritis, which might contribute to the prevention and treatment of the disease.

 doi:10.20944/preprints202404.1170.v1

2. Materials and Methods

2.1. Ethics Statement

The sampling method and all subsequent methods were approved by the Ethics Committee of Hainan University (Haikou, China, Permit No. HNUAUCC-2023-00080). This experiment did not involve endangered or protected species.

2.2. Animal Experiments

A total of eighteen fourteen-day-old Wenchang chickens (purchased from Hainan Taniu Wenchang Chicken Co.) were randomly divided into three groups (n=6). The CON group was the healthy control group. The SAL group was infected with *Salmonella Typhimurium* (*S Typhimurium*) on day 23. The ABX group was administered a cocktail of antibiotics containing ampicillin (1 g/L), neomycin sulfate (1 g/L), metronidazole (1 g/L), and vancomycin (0.5 g/L) via drinking water from days 7 to 21; on day 22, this group was given regular drinking water and infected with *S. Typhimurium* on day 23 (Figure 1). All the chickens were fed the same diet and had free access to food and water. The beginning of the experiment was counted as day 0, and the entire experiment lasted 30 days. Infection was by gavage and the infection measure was 1×10^9 CFU of *S. Typhimurium* per chicken. The strain was *Salmonella enterica serovar Typhimurium* (strain no. ATCC14028). The three groups of chickens were kept in three separate rooms with the same temperature, humidity, and other conditions to avoid cross-infection. At 3-4 weeks of age, the temperature was 28-30 °C, the relative humidity was 55%-60%, and the illumination time was 16 hours; at 5-6 weeks of age, the temperature was 24-26 °C, the relative humidity was 50%-55%, and the light time was 12 hours. Chickens were fed in cages with dimensions of 120 cm × 60 cm × 45 cm. All chickens were euthanized by cervical dislocation on day 30, and cecum contents and cecal intestinal tissue were collected aseptically on ice for subsequent analysis.

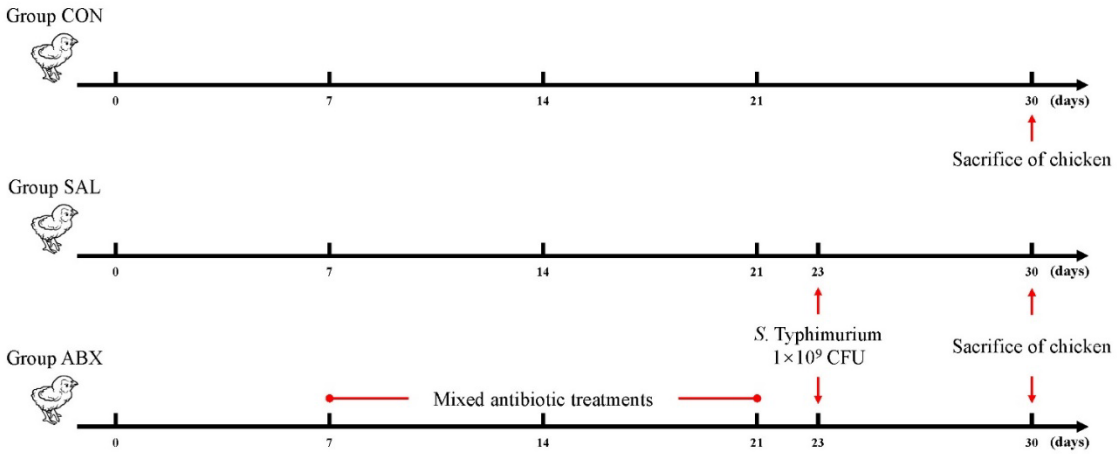

Figure 1. Schematic diagram of chicken grouping and experimental procedure.

2.3.16. s rDNA Sequencing and Data Analysis

The DNA was extracted using the CTAB (hexadecyl trimethyl ammonium bromide) method according to the manufacturer's instructions. PCR amplification was used to construct libraries for sequencing. Briefly, amplification was performed using the specific primers listed in Table 1, and the PCR products were confirmed using 2% agarose gel electrophoresis, purified with AMPure XT beads

 doi:10.20944/preprints202404.1170.v1

(Beckman Coulter Genomics, Danvers, MA, USA), and quantified with Qubit (Invitrogen, USA) to obtain libraries for sequencing. The size and number of libraries were evaluated using Agilent 2100 Bioanalyzer (Agilent, USA) and Illumina (Kapa Biosciences, Woburn, MA, USA) library quantification kits, respectively. The libraries were sequenced on the NovaSeq PE250 platform. Quality raw reads were filtered under specific filtering conditions to obtain high-quality clean tags according to fqtrim (v0.94). Chimeric sequences were filtered using Vsearch software (v2.3.4) [13]. After dereplication using DADA2 [14], we obtained the feature table and sequence. Alpha and beta diversities were randomly calculated by normalizing to identical sequences. Then, according to the SILVA (Release 138) classifier [15], feature abundance was normalized using the relative abundance of each sample. QIIME2 was used to calculate beta diversity and alpha diversity (Chao1, observed species, Good's coverage index, Shannon, and Simpson) [16], and the R package was used to prepare the graphs. BLAST was used for sequence alignment, and the feature sequences were annotated using the SILVA database for each representative sequence. Other diagrams were drawn using the R package (v3.5.2, https://cran.r-hub.io/bin/windows/base/). This study's raw data were uploaded to the NCBI database under the number PRJNA1027078. Sequencing and data analysis were entrusted to Shanghai Biotree Biotech Co.

LDA effect size (LEfSe) analysis was used to find species that differed significantly in abundance between groups. First, the Kruskal-Wallis rank sum test was utilized to detect all characterized species, and significantly different species were identified by detecting differences in species abundance between different groups. Then, the Wilcoxon rank sum test was utilized to test whether all subspecies of the significantly different species obtained in the previous step converged to the same taxonomic level. Finally, linear discriminant analysis (LDA) was used to estimate the magnitude of the effect of species abundance on the differential effect to obtain the final differential species. The screening conditions for LDA were LDA > 4 and $P < 0.05$.

Table 1. PCR-specific amplification primer sequences.

Amplified fragments	Primer Sequences
V3-V4 [17]	F (5'-CCTACGGGNGGCWGCAG-3') R (5'-GACTACHVGGGTATCTAATCC-3')
V4 [18]	F (5'-GTGYCAGCMGCCGCGGTAA-3') R (5'- GGACTACHVGGGTWTCTAAT-3')
V4-V5	F (5′-GTGCCAGCMGCCGCGG-3′) R (5′-CCGTCAATTCMTTTRAGTTT-3′)
Archae [19]	F (5′-GYGCASCAGKCGMGAAW-3′) R (5′-GGACTACHVGGGTWTCTAAT-3′)

2.4. Metabolite Extraction and Standard Solution Preparation

Briefly, the intestinal tissues were treated with extract (80% methanol/H_2O (V/V), precooled at -40 °C, containing isotopically labeled internal standard mixture), purified via solid-phase extraction, dried through nitrogen blowing, re-solubilized with 30% acetonitrile, and then centrifuged at 4 °C and 12,000 rpm for 15 min to obtain the supernatant, which was subjected to UHPLC-MS/MS analysis.

Stock solutions were prepared by dissolving or diluting each standard substance to a final concentration of 1 μg/mL. An aliquot of each stock solution was transferred to an Eppendorf tube to obtain a mixed working standard solution. A series of traditional calibration solutions were then prepared through stepwise dilution of this mixed standard solution (containing the isotopically labeled internal standard mixture at identical concentrations to the samples). Table S2 lists the standards used in this assay.

2.5. UHPLC-MRM-MS Analysis

UHPLC separation was performed using an EXIONLC System (Sciex) equipped with a Waters ACQUITY UPLC BEH C18 column (150 × 2.1 mm, 1.7 μm, Waters). A SCIEX 6500 QTRAP+ triple

 doi:10.20944/preprints202404.1170.v1

quadrupole mass spectrometer (Sciex) equipped with an IonDrive Turbo V electrospray ionization interface was used for assay development. The MRM parameters for each target analyte were optimized using flow injection analysis by injecting standard solutions of individual analytes into the API source of the mass spectrometer. Several of the most sensitive transitions were used in MRM scan mode to optimize the collision energy for each Q1/Q3 pair (Table S3). Among the optimized MRM transitions per analyte, the Q1/Q3 pairs with the highest sensitivity and selectivity were selected as "quantifiers" for quantitative monitoring. The additional transitions acted as qualifiers to verify the identity of the target analyte. The SCIEX Analyst WorkStation Software (Version 1.6.3) and the Multiquant 3.03 software were used for MRM data acquisition and processing. Metabolite assays and data analysis were entrusted to Shanghai Biotree Biotech Co.

2.6. Metabolite Assay Results and Quality Control

The calibration solutions were sequentially diluted 2-fold and analyzed using UHPLC-MRM-MS. The lower limits of detection (LLODs) and quantification (LLOQs) of the methods were calculated using their signal-to-noise ratios. According to the United States Food and Drug Administration guidelines for bioanalytical method validation, the LLODs of a method are defined as the concentration of a compound with a signal-to-noise ratio of 3, and the LLOQs of a method are defined as the concentration of a compound with a signal-to-noise ratio of 10. Table S4 lists the resulting LLODs and LLOQs. The LLODs for the targeted metabolites ranged from 0.0195 to 1.2500 ng/mL, and the LLOQs ranged from 0.0390 to 2.5000 ng/mL. The correlation coefficients (R2) of regression fitting were above 0.9959 for the analytes, indicating a good quantitative relationship between the MS responses and analyte concentrations, satisfying the target metabolomics analysis. Table S5 lists the analytical recoveries and relative standard deviations of the QC samples with five technical replicates. The recoveries were 85.07–111.47% for all analytes, with all RSDs below 14.09% (n = 5). The analysis metrics indicated that the method allowed for the accurate quantitation of the targeted metabolites in the biological samples in the above concentration range.

The quantification results are presented in Table S6. The final concentration (cF, ng/mL) was equal to the calculated concentration (cC, ng/mL) multiplied by the dilution factor (Dil). For solid samples, the metabolite concentration (cM, ng/g) was equal to the final concentration (cF, ng/mL) multiplied by the final volume (VF, μL) and equal to the sample experiment concentration factor (CF) divided by the mass (m, mg) of the sample. N/A indicates that the targeted metabolites were not detectable in the corresponding samples.

2.7. Cell Experiments

2.7.1. Establishment of HD11 Cell Model Infected by *S. Typhimurium*

First, the lowest concentration of cyclooxygenase inhibitor (aspirin) that inhibited the growth of *S. Typhimurium* in vitro was determined. *S. Typhimurium* was cultured in an LB sterile liquid medium containing different aspirin concentrations for 6-8 hours, and the bacteria growth in each group was counted by the plate count method.

Varied concentrations of aspirin (0, 31.25, 62.5, 125, 200, 500, and 1000 μg/mL) were then applied to HD11 cells for different times (0, 12, and 24 hours). Cell viability was measured by MTT to determine the maximal aspirin concentration and treatment time.

Finally, HD11 cells were infected with *S. Typhimurium* at selected MOIs (1, 5, 10, 20, and 50). The relative expression levels of iNOS, IL-1β, IL-6, and IL-10 mRNA in the cells were measured to determine the appropriate MOIs and time of infection.

2.7.2. Chicken Grouping and Cell Experiments

HD11 cells were infected with *S. Typhimurium* for 2 hours (MOI = 20) after being pretreated with a medium with aspirin concentrations of 30, 60, and 120 μg/mL for 12 hours.

 doi:10.20944/preprints202404.1170.v1

2.8. Quantitative Real-Time Polymerase Chain Reaction (qRT-PCR) Analysis and ELISA ASSAY

Changes in specific cytokine mRNAs and ARA metabolites in cecum in vivo and HD11 cells in vitro following *S. Typhimurium* infection were assessed by qRT-PCR and ELISA. The cecum tissue was homogenized using an automated sample rapid grinder (Tissuelyser-24L, Shanghai Jingxin Industrial Development Co., Ltd., Shanghai, China), and total RNA was extracted from the cecum tissue using the TRIzol method. Total RNA was extracted from HD11 cells by the TRIzol method. cDNA was prepared by the TIANGEN cDNA synthesis kit. The qRT-PCR analysis was performed using SYBR Green Master Mix, and glyceraldehyde-3-phosphate dehydrogenase (GAPDH) was used as a housekeeping gene. The mRNA concentration of all samples was adjusted to 1000 ng/mL during reverse transcription. The primers used are listed in the Supplementary Materials (Table S1). The relative gene expression was calculated using the $2^{-\Delta\Delta Ct}$ method. GraphPad Prism (version 8.0c) and SPSS 17.0 were used for statistical analysis. Data were analyzed using the $2^{-\Delta\Delta Ct}$ method and expressed as mean ± standard error (SEM). The statistical significance of the data was assessed using a one-way analysis of variance (ANOVA) followed by Duncan's and Tukey's tests.

The ELISA kits were used to detect COX-2, PGF2α, PLA2, and ARA in the samples according to the instructions.

2.9. Statistical Analysis of Data

Metabolites from each group were normalized using the Z-score normalization method, which is indicated by the value of $(x-\mu)/\sigma$. "μ" denotes the mean of the overall data, "σ" denotes the standard deviation of the overall data, and "x" denotes the individual observation. The Z-score values were calculated using MedCalc 22 (https://www.medcalc.org/) software. R (3.4.4, https://cran.r-hub.io/bin/windows/base/old/3.4.4/) was used to create a plot of the Z-scores.

Spearman's correlation analysis was used to assess the correlation between three data types: oxidized fats, inflammatory factors, and intestinal flora. The Spearman correlation analysis was carried out using the Stats package (2.5.4, https://search.r-project.org/R/refmans/stats/html/00Index.html) for R (3.4.4).

Multivariate statistical analysis was used to calculate the variable importance in the projection (VIP) values and orthogonal projections to latent structure discriminant analysis (OPLS-DA). The Mann–Whitney U test was used to compare differences between two groups of samples with biological replicates; the Kruskal–Wallis test was used to compare differences between multiple groups of samples with biological replicates. Adonis and ANOSIM were used to test whether the differences between groups were significantly greater than those within groups and to determine whether the subgroups were significant. The Vegan package (2.5.4, https://cran.r-project.org/web/packages/vegan/index.html) for R (3.4.4) was used for the above data analysis.

The datasets were evaluated for normal distribution using the D'Agostino–Pearson test and presented as mean ± standard error of the mean (SEM). Statistical significance was determined with either a two-tailed unpaired Student's t-test (for two groups) or one-way ANOVA (for grouped comparisons). In datasets analyzed using ANOVA, the Bonferroni post hoc test was adopted. A p-value less than 0.05 was considered statistically significant. All statistical analysis was performed with Prism version 8.0 (GraphPad, La Jolla, CA, USA) and SPSS 17.0.

3. Results

3.1. DNA Sequence and Microbial Diversity Index Analysis

The total number of Amplicon Sequence Variants (ASVs) in the three groups was 7504, with 4172, 3366, and 2243 ASVs in the CON, SAL, and ABX groups, respectively (Figure S1A). The average number of ASVs in each group was 695, 561, and 374, respectively. The Good's coverage index values of all samples in the CON, SAL, and ABX groups exceeded 99% (Figure S1B), which indicates that this sequencing result was representative of the real situation of the samples. When the number of valid sequences exceeded 40,000, the dilution curve (rarefaction curve) tended to flatten, indicating

 doi:10.20944/preprints202404.1170.v1

that the amount of sequencing data was saturated and that the depth and quantity of sequencing met the requirements for analysis (Figure S1C). In addition, the rank abundance curves for each group of samples had a large span in the horizontal direction. They were relatively flat in the vertical direction, indicating good species richness and good homogeneity of the samples (Figure S1D). The above results suggest that the quality of the sequencing data obtained in this study was reliable and sufficient, and the results are authentic.

The results of the α-diversity analysis showed that the mean values of the Shannon index were 6.94±0.23, 8.07±0.41, and 7.49±0.19 for the CON, SAL, and ABX groups (Table 2). The Shannon, Simpson, and Chao1 indices were lower in the SAL and ABX groups than in the CON group (Figure 2A-C). The principal coordinate analysis (PCoA) results among the three groups showed that the groups were distinct from each other and that there were differences in the structure of colony composition between the groups (Figure 2D).

Table 2. The alpha diversity index of each sample.

Sample	Shannon	Simpson	Chao1
ABX1	7.16	0.97	804.74
ABX2	6.82	0.97	797.58
ABX3	7.00	0.97	715.65
ABX4	6.55	0.97	732.29
ABX5	7.16	0.98	790.71
ABX6	6.96	0.97	754.43
CON1	7.60	0.98	1026.35
CON2	7.56	0.98	1029.39
CON3	8.16	0.99	1179.45
CON4	8.13	0.99	1148.30
CON5	8.52	0.99	1430.61
CON6	8.47	0.99	1373.35
SAL1	7.69	0.99	1105.00
SAL2	7.47	0.98	1018.76
SAL3	7.26	0.98	887.71
SAL4	7.68	0.98	1171.02
SAL5	7.27	0.97	1064.23
SAL6	7.58	0.99	916.28

Preprints.org (www.preprints.org) | NOT PEER-REVIEWED | Posted: 17 April 2024 doi:10.20944/preprints202404.1170.v1

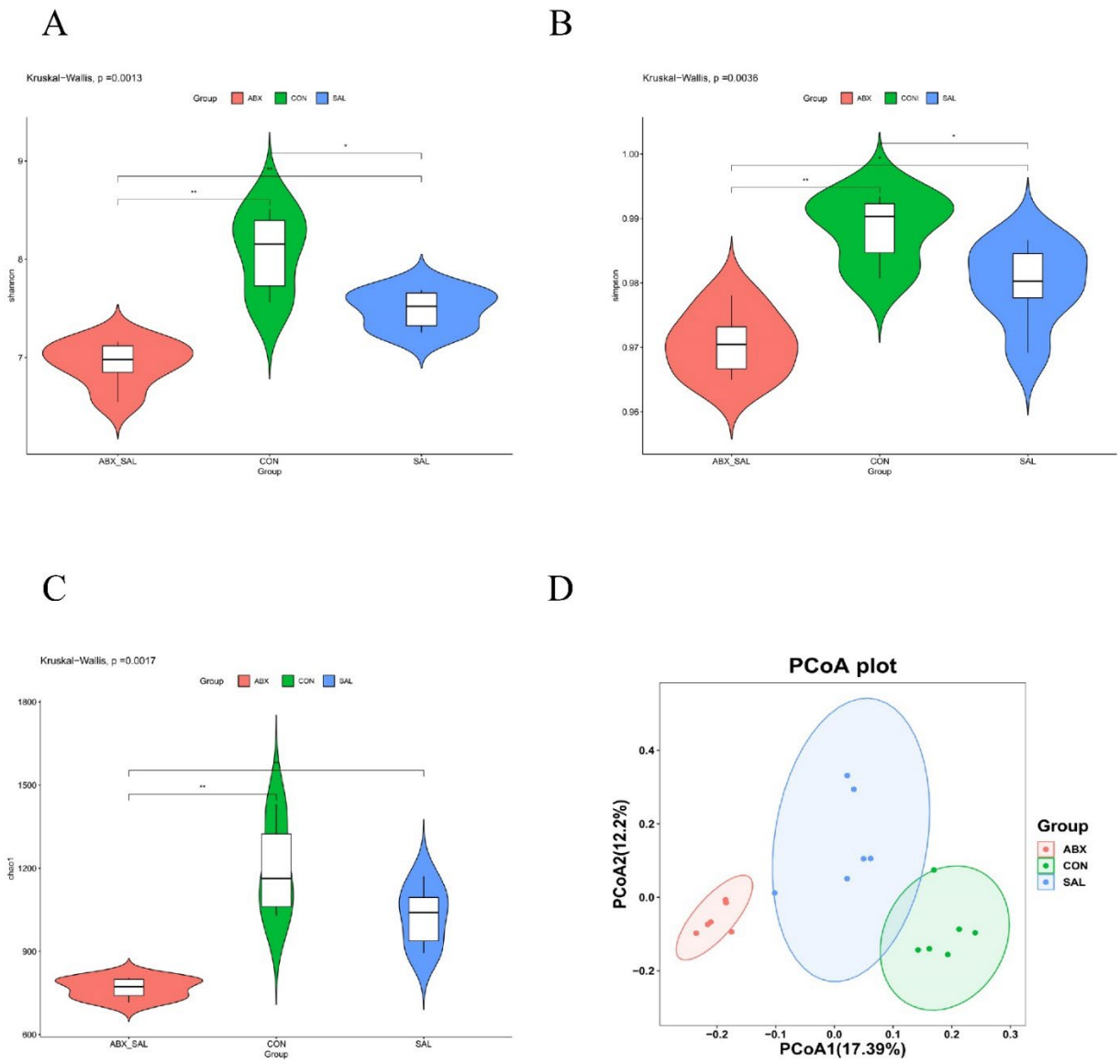

Figure 2. Results of difference analysis of cecum microbial communities between groups. (A) Shannon index. (B) Simpson's index (C) Chao 1 index. (**D**) PCoA analysis results. Different colors represent different groups. The closer the samples are, the more similar the microbial composition is between the samples.

3.2. Analysis of the Composition of the Intestinal Microbial Community

At the phylum level (Figure 3A and B), compared to the CON group, the relative abundance of *Cyanobacteria* (0.11%) and *Planctomycetota* (0.002%) in the SAL group decreased ($P < 0.05$), whereas the relative abundance of *Bacteroidota* (28.61%) and *Desulfobacterota* (1.04%) increased ($P < 0.05$). Compared to the CON group, the relative abundance of *Proteobacteria* (2.12%), *Actinobacteria* (1.45%), and *Cyanobacteria* (0.06%) in the ABX group decreased ($P < 0.05$), whereas the relative abundance of *Desulfobacterota* (2.51%) increased ($P < 0.05$). For information on the abundance of the top 30 species at the level of phylum, order, family, and genus, refer to Table S7. For information on differential species at the phylum and genus levels, refer to Table S8.

At the genus level (Figure 3C, D), compared to the CON group, the relative abundance of 26 genera was increased in the SAL group ($P < 0.05$, e.g., *Prevotellaceae_UCG001*, *Megasphaera*, and *Barnesiella*), and 40 genera were decreased ($P < 0.05$, e.g., *Lactobacillus*, *Streptococcus*, and

 doi:10.20944/preprints202404.1170.v1

Bifidobacterium). Compared to the CON group, the relative abundance of 24 genera was increased in the ABX group ($P < 0.05$, e.g., *Clostridium*, *Prevotellaceae_UCG-001*, and *Barnesiella*), and 79 genera were decreased ($P < 0.05$, e.g., *Faecalibacterium*, *Clostridia_UCG-014_unclassified*, and *Lactobacillus*). Compared to the CON group, 9 identical genera had significantly higher relative abundance in both the SAL and ABX groups, accounting for 34.62% of the SAL group and 37.50% of the ABX group, respectively. Compared to the CON group, 25 identical genera had significantly lower relative abundance in both the SAL and ABX groups, accounting for 62.50% of the SAL group and 31.65% of the ABX group, respectively.

The linear discriminant analysis (LDA) showed that three phyla (e.g., Actinobacteriota, Bacteroidota, and Desulfobacterota) and nine genera (e.g., Clostridia_UCG_014_unclassified, Faecalibacterium, Lactobacillus, Eubacterium_coprostanoligenes_group_unclassified, Prevotellaceae_UCG_001, Megasphaera, HT002, Barnesiella, and Clostridium) were significantly different between groups ($P < 0.05$) (Figure S2). The phylum Bacteroidota and the genus Prevotellaceae_UCG_001 had the highest LDA scores at the phylum and genus level, respectively, suggesting that they had a greater influence on the differences between groups.

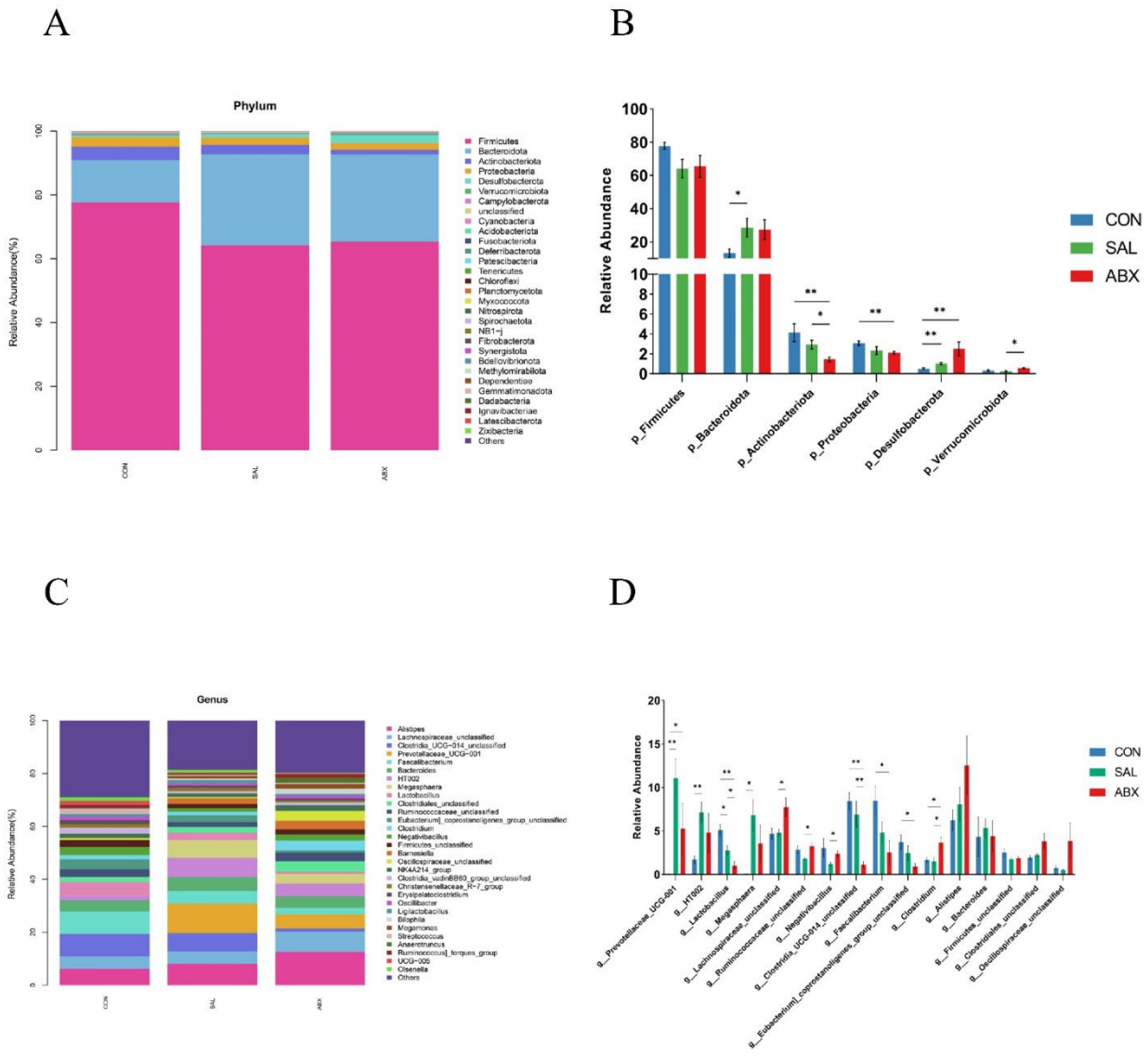

Figure 3. Taxonomic distribution of the CON, SAL, and ABX groups. (**A**) At the phylum level (top 30). (**B**) Differences in the partially dominant bacterial flora at the phylum level among the groups. (**C**) At the genus level (top 30). (**D**) Differences in the partially dominant bacterial flora at the genus

 doi:10.20944/preprints202404.1170.v1

level among the groups. "*" indicates a significant difference in statistics (*$P < 0.05$, **$P < 0.01$, and ***$P < 0.001$).

3.3. Salmonella Typhimurium Infection Affects Polyunsaturated Fatty Acid Metabolism in Intestinal Tissues

A total of 130 oxidized lipid metabolites were detected from 18 cecum tissue samples, and 71 metabolites were retained after preprocessing (Table S9). These included thirty-seven mid-ARA metabolites, eight docosahexaenoic acid (DHA) metabolites, eight linoleic acid (LA) metabolites, five dihomo-γ-linolenic acid (DGLA) metabolites, five eicosapentaenoic acid (EPA) metabolites, two α-linolenic acid (ALA) metabolites, one docosatetraenoic acid (DTA) metabolite, and one gamma-linolenic acid (GLA) metabolite.

The results of principal component analysis (PCA) for the 71 metabolites showed that the samples from the ABX and SAL groups were distinct from the samples from the CON group, and the samples from the ABX and SAL groups were not completely separated (Figure 4 and S3). The multiplicity of differences between the top 20 metabolites that were increased and the top 20 metabolites that were decreased in each comparison group (SAL vs. CON, ABX vs. CON, and ABX vs. SAL) are shown in Figure 5A-C. The Z-score for each comparison group is shown in Figure S4. The results of the cluster analysis of metabolites in each group are shown in Figure S5. The above results visually indicated that the content of multiple oxidized lipid metabolites was altered in the cecum tissues of the SAL group.

 doi:10.20944/preprints202404.1170.v1

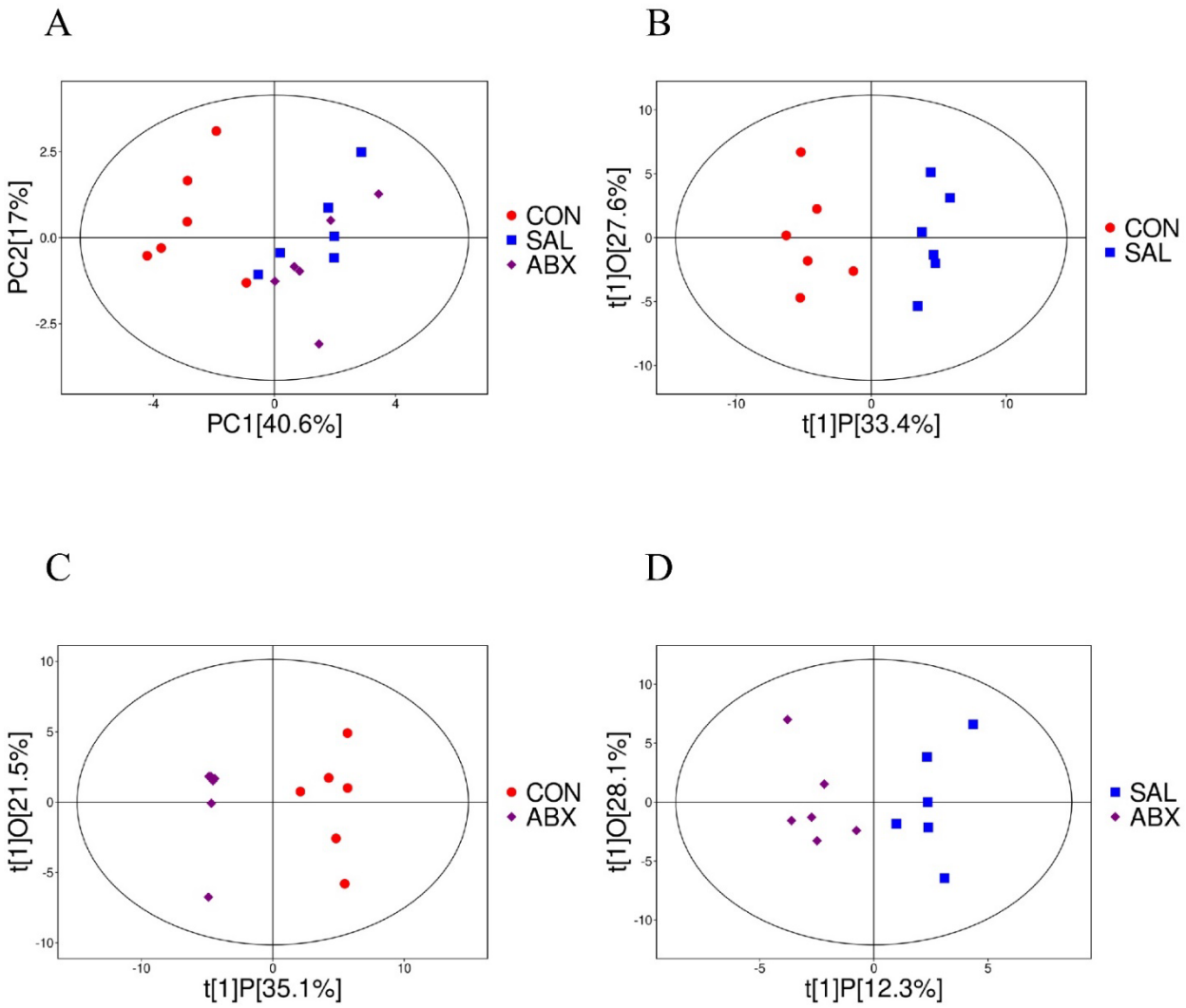

Figure 4. Analysis of PCoA and OPLS-DA between the CON, SAL, and ABX groups. (**A**) Scatterplot of principal component analysis (PCA) scores for the full sample in each group. (**B**, **C**, **D**) Scatterplot of OPLS-DA model scores between groups. The horizontal coordinate represents the predicted principal component scores of the first principal component, demonstrating the differences between sample groups, whereas the vertical coordinate represents the orthogonal principal component scores, demonstrating the differences within the sample groups, where each scatter represents one sample and the scatter shapes and colors indicate the different experimental groups.

 doi:10.20944/preprints202404.1170.v1

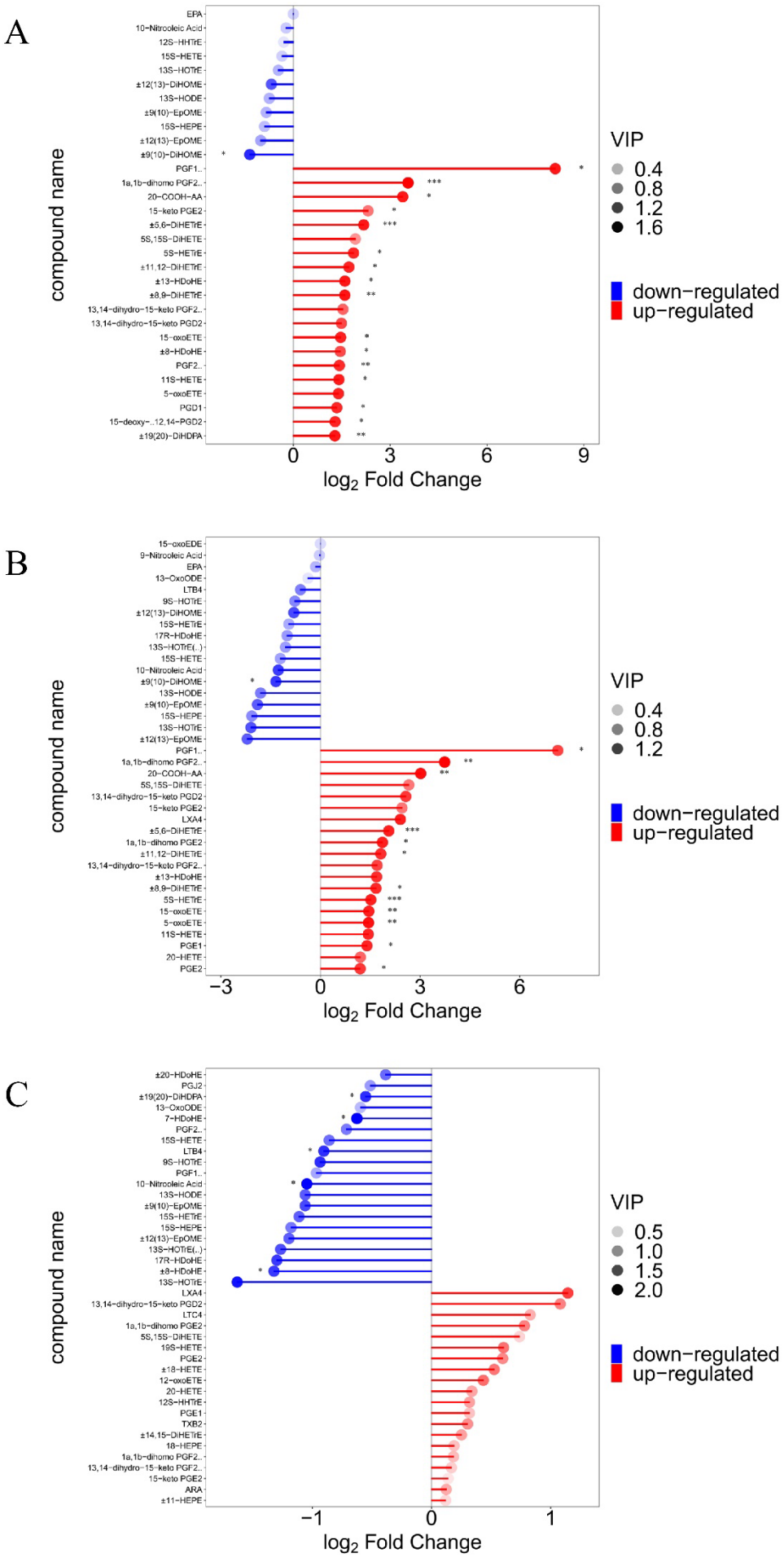

 doi:10.20944/preprints202404.1170.v1

Figure 5. Demonstration of differences in oxygenated lipid metabolites between groups. (A, B, C) Matchstick analysis for three comparison groups (SAL vs. CON, ABX vs. CON, and ABX vs. SAL). Horizontal coordinates show logarithmically converted multiples of change, with point color shades representing the size of the variable importance in the projection (VIP) value. "*" indicates a significant difference in statistics (*$P < 0.05$, **$P < 0.01$, and ***$P < 0.001$).

3.4. Overall Enhancement of Arachidonic Acid Metabolism in Chicken Cecum Tissue Caused by Salmonella Typhimurium Infection

In this experiment, the groups were screened for differential metabolites with a p-value of less than 0.05 (Table S10). The results showed that 26 metabolites were significantly higher ($P < 0.05$) and one significantly lower (±9(10)-DiHOME) in the SAL group compared to the CON group ($P < 0.05$), for a total of 27 metabolites that were significantly changed. These included fifteen ARA metabolites, three DGLA metabolites, six DHA metabolites, one LA metabolite, and one DTA metabolite. Of the fifteen ARA differential metabolites in the SAL group, two were COX metabolic pathway products (e.g., PGF2α and 15-keto-PGE_2), two belonged to the LOX pathway (e.g., LXA4 and 15-OxoETE), and six belonged to the CYP metabolic pathway (e.g., ±11(12)-EET, ±8(9)-EET, ±14,15-DiHETrE, ±11,12-DiHETrE, ±8,9-DiHETrE, and ±5,6-DiHETrE). The results are displayed in the Kyoto Encyclopedia of Genes and Genomes (KEGG) pathway enrichment analysis plot (Figure S6A).

There were 22 metabolites with significantly higher levels ($P < 0.05$) and one with a significantly lower level (±9(10)-DiHOME) in the ABX group compared to the CON group ($P < 0.05$), for a total of 23 metabolites that were significantly changed. These included 15 ARA metabolites, three DGLA metabolites, one DHA, one LA metabolite, and one DTA metabolite. Of the 15 ARA differential metabolites in the ABX group, one was a product of the COX metabolic pathway product (e.g., PGE_2), three belonged to the LOX pathway (e.g., 5S-HETE, 5-oxoETE, and 15-OxoETE), and six belonged to the CYP metabolic pathway (e.g., ±11(12)-EET, ±8(9)-EET, ±14,15-DiHETrE, ±11,12-DiHETrE, ±8,9-DiHETrE, and ±5,6-DiHETrE). The results are displayed in the KEGG pathway enrichment analysis (Figure S6B). Fifteen of the differential metabolites were found to be identical in the SAL and ABX groups, accounting for 55.56% and 68.2% of these groups, respectively. Differences in ARA metabolites between groups are presented as bar graphs (Figure 6).

 doi:10.20944/preprints202404.1170.v1

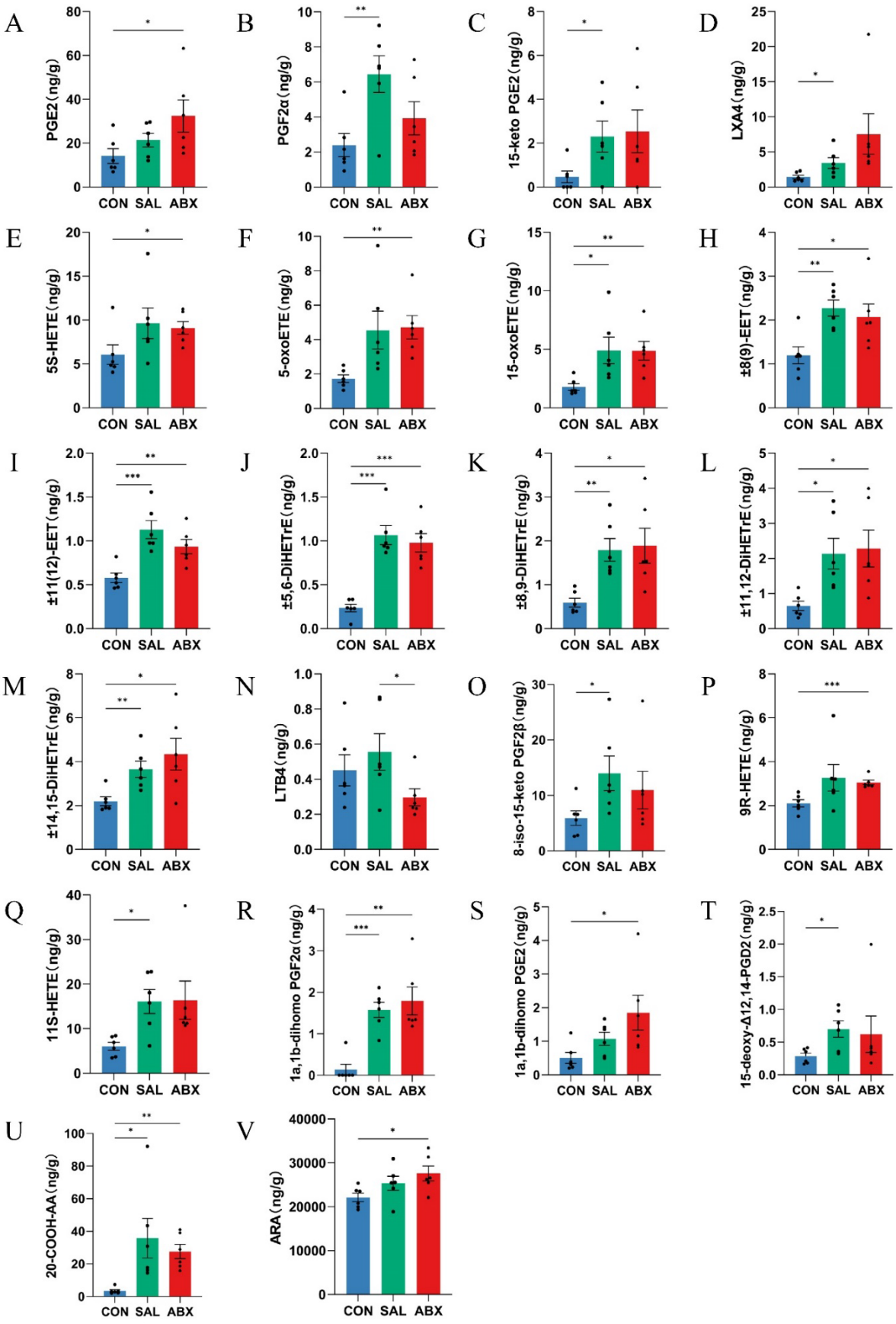

Figure 6. Analysis of between-group differences in ARA metabolites. "*" indicates a significant difference in statistics (*$P < 0.05$, **$P < 0.01$, and ***$P < 0.001$).

 doi:10.20944/preprints202404.1170.v1

3.5. Spearman Analysis Results between Oxidized Lipid Metabolites, Intestinal Flora, and Inflammatory Factors

The relative mRNA levels of IL-4 and transforming growth factor-beta 1 (TGF-β1) were increased in the SAL group compared with the CON group ($P < 0.05$), and there was a trend toward higher levels of IL-6 ($P > 0.05$) (Figure S7). Relative mRNA levels of interferon-gamma (IFN-γ), IL-4, TGF-β1, and IL-6 were increased ($P < 0.05$), and IL-2 levels were decreased ($P < 0.05$) in the ABX group compared with the CON group (Figure S7). Tumor necrosis factor-alpha (TNF-α), IL-4, TGF-β1, IFN-γ, and IL-6 levels were higher ($P < 0.05$) in the ABX group than in the SAL group, and IL-2 and interleukin 1β (IL-1β) levels were lower ($P < 0.05$) in the ABX group than in the SAL group (Figure S7). The results of the "Spearman" analysis between oxidized lipid metabolites, intestinal flora, and inflammatory factors are shown in Figure 7, Table S11, and Table S12.

 doi:10.20944/preprints202404.1170.v1

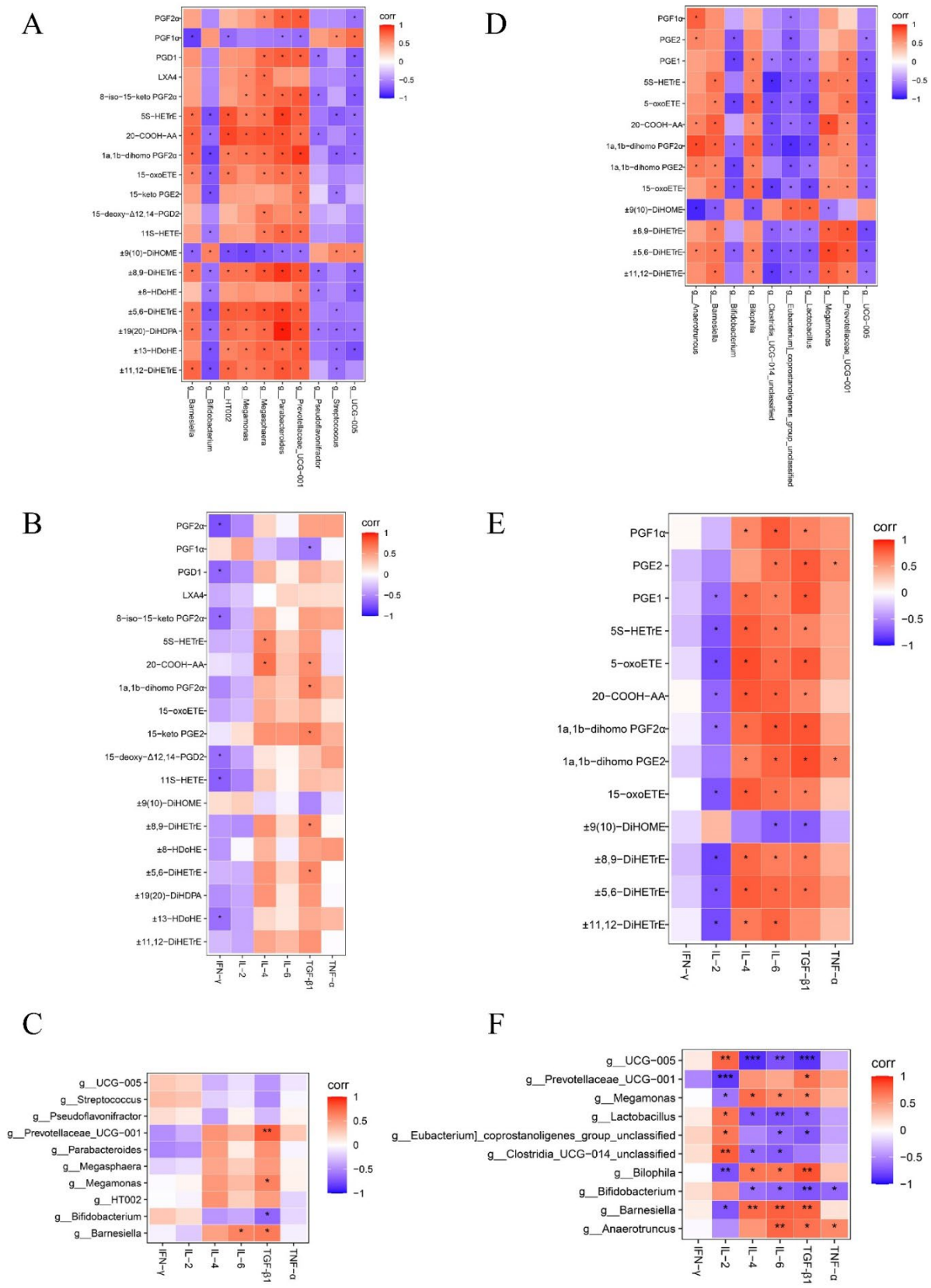

Figure 7. Heatmap of correlation coefficient matrix for the SAL and ABX groups. (**A**, **B**, **C**) Analysis of Spearman's correlation between oxidized lipid metabolites, gut microbes, and inflammatory factors in the SAL group. (**D**, **E**, **F**) Analysis of Spearman's correlation between oxidized lipid metabolites, gut microbes, and inflammatory factors in the ABX group. Red indicates a positive correlation, and

 doi:10.20944/preprints202404.1170.v1

purple indicates a negative correlation. "*" indicates a significant difference in statistics (*$P < 0.05$, **$P < 0.01$, and ***$P < 0.001$).

3.6. Salmonella Typhimurium Infection activates the Cyclooxygenase Metabolic Pathway of Arachidonic Acid

The results of cellular experiments showed that aspirin pretreatment did not significantly affect the relative expression levels of IL-1β, IL-6, and IL-10 mRNA in HD11 cells compared with the untreated group (Figure 8A-C). However, the iNOs were significantly increased in HD11 cells after treatment with 60 and 120 μg/mL aspirin and strengthened with the increase of aspirin concentration (Figure 8D). Compared to the untreated group, relative mRNA levels of IL-1β, IL-6, IL-10, and iNOs were increased in HD11 cells after *S. Typhimurium* infection ($P < 0.001$). Whereas aspirin pretreatment reduced this effect in a dose-dependent manner. The results of cellular experimental modeling and drug concentration screening are shown in Figures S8 and S9.

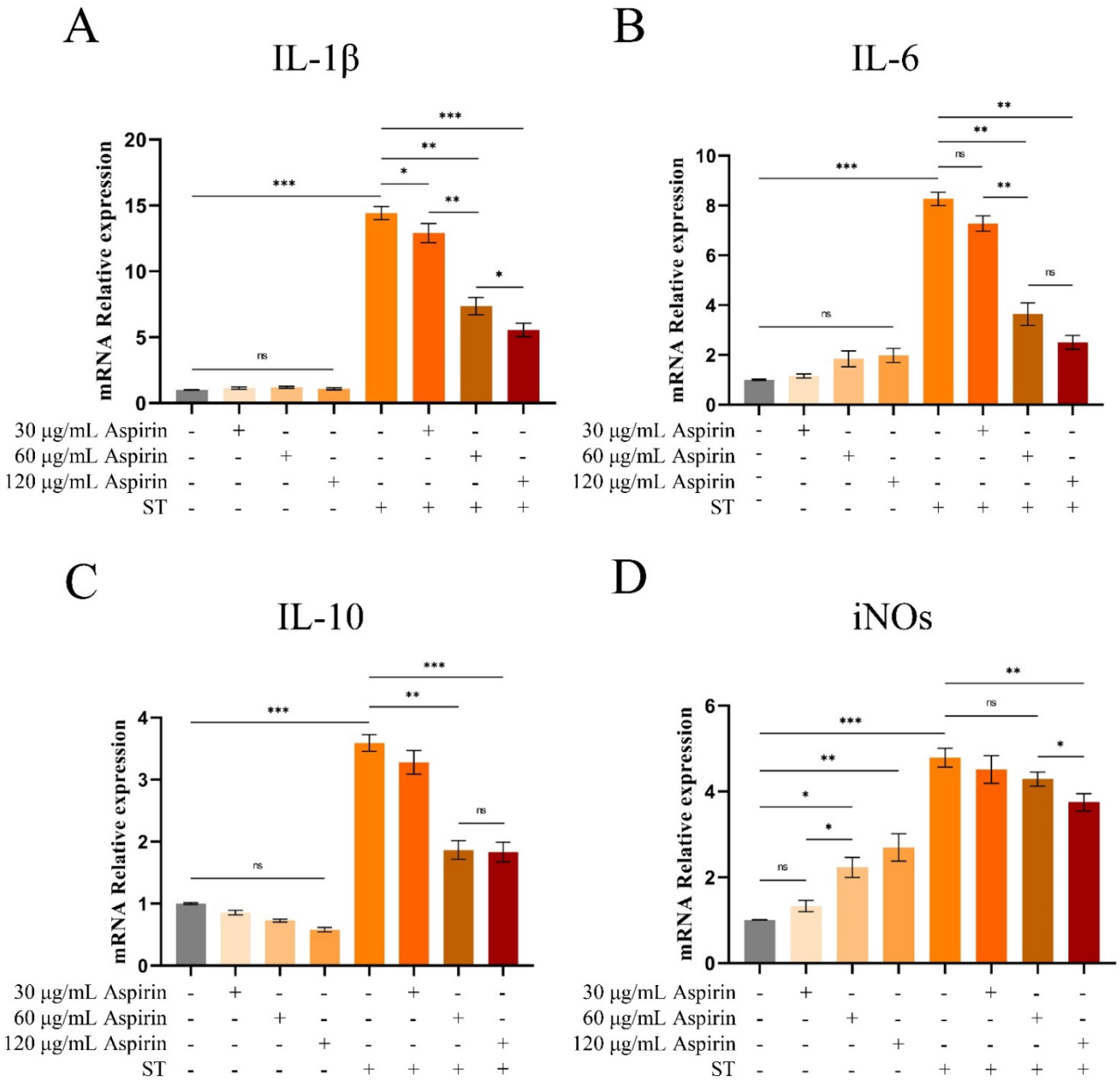

 doi:10.20944/preprints202404.1170.v1

Figure 8. Changes in IL-1β, IL-6, IL-10 and iNOs in HD11 cells. "*" indicates a significant difference in statistics (*$P < 0.05$, **$P < 0.01$, and ***$P < 0.001$).

3.7. Salmonella Typhimurium Infection Activates the Cyclooxygenase Metabolic Pathway of Arachidonic Acid

The levels of COX-2 and PLA2 in cecum tissues were increased in both the SAL and ABX groups after *S. Typhimurium* infection compared to the CON group ($P < 0.05$ or $P < 0.01$) and did not differ between either the SAL and ABX groups (Figure 9A-D). Compared to the CON group, the levels of ARA in cecum tissues and cecum contents were increased in both the SAL and ABX groups after *S. Typhimurium* infection ($P < 0.05$), and there was no difference between the SAL and ABX groups (Figure 9E-F).

Compared to the untreated group, aspirin pretreatment had no significant effect on the levels of COX-2 in HD11 cells (Figure 10A-B), but the relative mRNA expression level of PLA2 was significantly increased when the concentration reached 60 and 120 μg/mL ($P < 0.05$) with a dose-dependent trend (Figure 10D). Compared to the untreated group, aspirin pretreatment had no significant effect on the levels of PLA2, PGF2α, and ARA in HD11 cells (Figure 10C, E, and F).

Compared to the untreated group, the relative mRNA expression level of COX-2 in HD11 cells was increased after *S. Typhimurium* infection ($P < 0.001$), whereas aspirin pretreatment significantly reduced this effect (Figure 10B, $P < 0.05$ or $P < 0.01$). Meanwhile, Elisa's results showed that COX-2 content in HD11 cells was increased after *S. Typhimurium* infection ($P < 0.05$). However, aspirin pretreatment could not inhibit the increased COX-2 content induced by infection (Figure 10A). Compared to the untreated group, PGF2α content in HD11 cells was increased after *S. Typhimurium* infection ($P < 0.05$). However, aspirin pretreatment (120 μg/mL) reduced the infection-induced increases in PGF2α content (Figure 10F $P < 0.05$). Compared to the untreated group, the levels of ARA and PLA2 in HD11 cells did not change significantly after *S. Typhimurium* (Figure 10C and E).

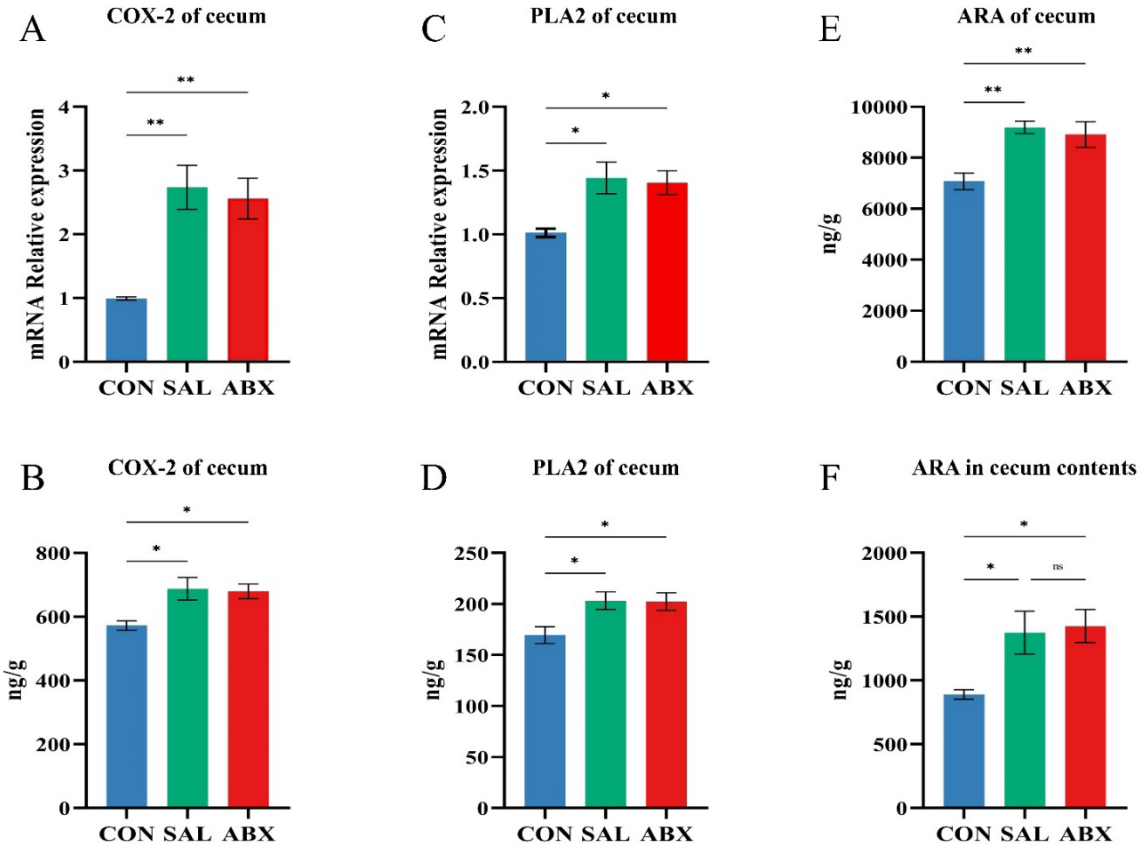

Figure 9. Changes of arachidonic acid and its key enzymes of metabolic pathway in the cecum. (A-D) COX-2 and PLA2 content and relative mRNA expression levels in cecum tissues. (E, F) ARA content

 doi:10.20944/preprints202404.1170.v1

in cecum tissues and cecum contents. "*" indicates a significant difference in statistics (*P < 0.05, **P < 0.01, and ***P < 0.001).

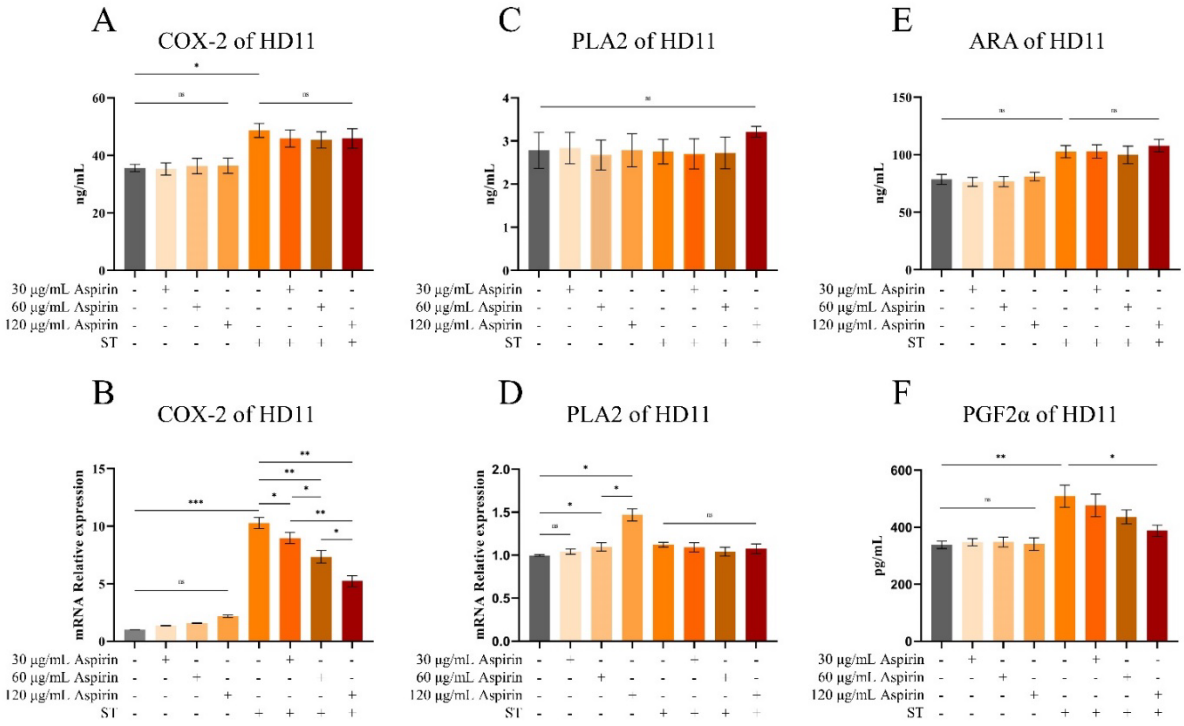

Figure 10. Changes of arachidonic acid and its key enzymes of metabolic pathway in HD11 cells. "*" indicates a significant difference in statistics (*P < 0.05, **P < 0.01, and ***P < 0.001).

4. Discussion

Intestinal inflammation caused by avian salmonellosis is necessary for *Salmonella* colonization and survival [2]. Arachidonic acid (ARA) metabolites are an important and widely acting class of inflammatory mediators [20]. Therefore, the relationship between arachidonic acid metabolites and *Salmonella* enteritis would be beneficial for the prevention and treatment of the disease.

PLA2 and COX-2 are key enzymes for ARA production and metabolism [21,22], respectively. *Salmonella Typhimurium* (*S. Typhimurium*) infection caused increased levels of PLA2 and COX-2 in the intestinal tissues of Wenchang chickens, which may be the direct cause of the increased levels of arachidonic acid and its metabolites in the cecum tissues. A number of studies have shown that ARA metabolites (e.g., prostaglandins, leukotrienes, and lipoxins) mediate inflammatory responses in the intestine via different types of G-protein-coupled receptors [23–26]. For example, PGE_2 signals through prostaglandin E receptor 2 (EP2) on neutrophils and tumor-associated fibroblasts, which promotes inflammation through multiple steps to form the tumor microenvironment in colorectal cancer [27] and induces mast cell activation through the EP3 receptor signaling pathway, which enhances vascular permeability and promotes acute inflammation [28]. PGF2α levels are significantly increased in patients with ulcerative enteritis, which is alleviated by the use of PLA2 inhibitors [29]. 5-OxoETE (precursor of 5(S)-HETE) promotes the basophil migratory response [30], and is involved in neuroinflammatory activities [31]. LXA4 facilitates the reduction in chronic inflammation, inhibits the production of PGE_2 and LTs, and suppresses the production of pro-inflammatory factors IL-6 and TNF-α [32]. 15-OxoETE can activate anti-inflammatory Nrf2 signaling and inhibit the NF-κB-mediated pro-inflammatory pathway [33]. EETs (e.g., 8,9-EET, 11,12-EET) prevent leukocyte adherence to the vascular wall through inhibition of the transcription factors NF-κB and IκB kinase and play an important non-vasodilatory role in vascular inflammation [34]. EETs can also inhibit the

 doi:10.20944/preprints202404.1170.v1

activation of NOD-like receptor thermal protein domain associated protein three inflammatory vesicles by suppressing calcium overload and reactive oxygen species production in macrophages, thereby facilitating the treatment of acute lung injury [35]. It is thus evident that arachidonic acid metabolites have both anti-inflammatory and pro-inflammatory effects. We speculate that arachidonic acid metabolites are key substances mediating avian *Salmonella* enteritis.

Prostaglandins such as PGE2 and PGF2α are metabolized by ARA by the COX-2 pathway [36]. We found that *S. Typhimurium* infection significantly increased the levels of COX-2 and PGF2α in HD11 cells and promoted the mRNA expression of inflammatory factors (IL-1β, IL-6, and iNOs). Furthermore, a cyclooxygenase inhibitor (aspirin) significantly inhibited the inflammatory response induced by *S. Typhimurium* infection. This validates our conjecture, suggesting that the ARA cyclooxygenase metabolic pathway mediates the inflammatory response upon *S. Typhimurium* infection. Unfortunately, this study did not examine how ARA metabolites mediate the development and progression of avian *Salmonella* enteritis. This is because many of the metabolites have not been studied in vivo or in vitro in poultry, and some of the metabolites (e.g., EETs and PGE_2) are rapidly degraded to low effectors in the organism, making it difficult to control the experimental variables [37]. Therefore, it is necessary to explore the research conditions further, find suitable experimental methods for validation, and gradually explore the mechanism of action of the ARA metabolites in *Salmonella*-induced intestinal inflammation in the future.

Gut microbiota composition is one of the most important factors affecting animal intestinal immunity and serves as a barrier against invasion by pathogenic microorganisms. Infection with *S. Typhimurium* significantly reduced the number of microorganisms, the flora abundance, and the species diversity in the cecum of Wenchang chickens. This is similar to the changes in the intestinal flora of laying hens after *Salmonella* infection [38]. Notably, the abundance of many beneficial bacteria (*Bifidobacterium*, *Lactobacillus*, and *Odoribacter*) was significantly reduced in the SAL and ABX groups. Many studies have confirmed the beneficial effects of Bifidobacterium in animals. It prevents diarrhea [39], alleviates the symptoms of irritable bowel syndrome [40], prevents colorectal cancer [41], alleviates clinical signs in patients with ulcerative colitis [42], and regulates and maintains the structure of the intestinal flora [43]. Lactobacillus is a group of beneficial intestinal bacteria that can prevent Clostridium difficile-infection-associated diarrhea [44], facilitate intestinal inflammation [45], and regulate immune-related molecules to enhance intestinal barrier function [46,47].

The Spearman analysis showed a significant positive correlation between the relative abundance of *Bifidobacterium* and *Lactobacillus* and the relative mRNA expression of IL-2 in intestinal tissues ($P < 0.05$). IL-2 is a cytokine essential for the growth and survival of regulatory T cells (Tregs) in peripheral lymphoid tissues. Tregs are essential for the maintenance of peripheral tolerance and for the control of persistent inflammation and autoimmunity [48]. However, the relative mRNA content of IL-2 in the intestinal tissues of Wenchang chickens tended to decrease after S. Typhimurium infection. This suggests that avian gut microbiota, especially beneficial bacteria, potentially regulate intestinal immunity. However, *Salmonella* infection reduces the abundance of beneficial flora, which in turn reduces the immune function of the intestine, leading to the overgrowth of certain inflammation-associated genera in the avian intestinal tract, further aggravating intestinal inflammation. This suggests that probiotics or other beneficial substances can be appropriately added to feed to regulate the flora structure and improve resistance to harmful microorganisms [49–51]. For example, *Odoribacter* has shown promise as a next-generation probiotic that improves glucose tolerance and obesity-associated inflammation [52]. *Lactofructose* attenuated colitis symptoms by upregulating *Muribaculum* abundance [53]. An inevitable problem in this study was that it was not possible to experimentally verify these results. This is because the gut microbial system is too complex to control these variables.

In summary, this study found that infection with *S. Typhimurium* resulted in disturbed intestinal flora and a significant activation of ARA metabolism in Wenchang chickens. It also reported some ARA metabolites to be involved in the induction of inflammation. Given that the inflammatory intestinal environment is conducive to colonization and invasion by *Salmonella*, it is suggested that

 doi:10.20944/preprints202404.1170.v1

modulating ARA metabolism in intestinal tissues may be a potential approach to control avian *Salmonella* enteritis.

5. Conclusions

This study found that *S. Typhimurium* infection induced levels of several arachidonic acid metabolites in chicken cecum tissues. In HD11 cells, a cyclooxygenase inhibitor significantly reduced the inflammatory response induced by *S. Typhimurium* infection. In addition, we observed the presence of disturbed cecal intestinal flora in the infected group, but the effect of this phenomenon on ARA metabolism was not significant. The above results suggest that *S. Typhimurium* can mediate the onset and development of intestinal inflammation by activating the chicken ARA cyclooxygenase metabolic pathway. These findings may provide new insights into how *Salmonella* induces avian *Salmonella* enteritis. Based on this study, potential new mechanisms for combating avian *Salmonella* enteritis can be further explored.

Supplementary Materials: The following supporting information can be downloaded at the website of this paper posted on Preprints.org, Figure S1: DNA sequence data analysis; Figure S2: Significant differences in bacterial taxa between groups were determined by linear discriminant analysis and effect size (LEfSe); Figure S3: Histogram of replacement test results for OPLS-DA model; Figure S4. Relative values of the Z-score for the three comparison groups (SAL vs. CON, ABX vs. CON, and ABX vs. SAL); Figure S5: Results of metabolite cluster analysis; Figure S6: KEGG enrichment pathway map of the differential metabolites in the SAL and ABX groups; Figure S7: Relative mRNA levels of inflammatory factors in cecum tissue; Figure S8. Effect of different concentrations of aspirin at different treatment times on the activity of HD11 cells and *S. Typhimurium*.; Figure S9. Effect of different infection multiplicities of *S. Typhimurium* on inflammation-related gene expression in HD11 cells within a time gradient; Table S1: qRT-PCR primer information; Table S2: Targeted analyte information; Table S3: MRM Parameters; Table S4: Calibration; Table S5: Recovery and RSD; Table S6: Quantification Results; Table S7: Abundance information for the top 30 species; Table S8: Species information on differences at the phylum and genus levels; Table S9: Information on the 71 retained metabolites; Table S10: Differential metabolite information by group; Table S11: Correlation coefficients between components of the SAL group; Table S12: Correlation coefficients between components of the ABX group.

Author Contributions: Conceptualization, S.C.; methodology, S.C.; validation, Y.X.; formal analysis, S.C.; investigation, S.C.; resources, X.W. and X.R.; data curation, D.G., T.L. and Z.T.; writing—original draft preparation, S.C.; writing—review and editing, S.C.; visualization, S.C. and Y.X.; supervision, X.W. and X.R.; project administration, X.W. and X.R.; funding acquisition, X.W. and X.R. All authors have read and agreed to the published version of the manuscript.

Funding: Please add: This research was funded by the National Natural Science Foundation of China (No. 32360878), the Natural Science Foundation of Hainan Province (No. 321RC1020), and the earmarked fund for the Hainan Agricultural Production Research System (No. HNARS-06-G05).

Institutional Review Board Statement: The sampling method and all subsequent methods were approved by the Ethics Committee of Hainan University (Haikou, China, Permit No. HNUAUCC-2023-00080). This experiment did not involve endangered or protected species.

Informed **Consent Statement:** Not applicable.

Data Availability Statement: The raw data of this study were uploaded to the NCBI database under the number PRJNA1027078.

Acknowledgments: We thank Shanghai Biotree Biotech Co., Ltd, for providing technical support for 16S sequencing and targeted metabolomics.

Conflicts **of Interest:** The authors declare no conflict of interest.

References

1. Fàbrega, A.; Vila, J. Salmonella enterica serovar Typhimurium skills to succeed in the host: virulence and regulation. Clin Microbiol Rev 2013, 26, 308-341, doi: 10.1128/cmr.00066-12

 doi:10.20944/preprints202404.1170.v1

2. Winter, S.E.; Thiennimitr, P.; Winter, M.G.; Butler, B.P.; Huseby, D.L.; Crawford, R.W.; Russell, J.M.; Bevins, C.L.; Adams, L.G.; Tsolis, R.M.; et al. Gut inflammation provides a respiratory electron acceptor for Salmonella. Nature 2010, 467, 426-429, doi: 10.1038/nature09415
3. El-Saadony, M.T.; Salem, H.M.; El-Tahan, A.M.; Abd El-Mageed, T.A.; Soliman, S.M.; Khafaga, A.F.; Swelum, A.A.; Ahmed, A.E.; Alshammari, F.A.; Abd El-Hack, M.E. The control of poultry salmonellosis using organic agents: an updated overview. Poult Sci 2022, 101, 101716, doi: 10.1016/j.psj.2022.101716
4. Han, Z.; Willer, T.; Li, L.; Pielsticker, C.; Rychlik, I.; Velge, P.; Kaspers, B.; Rautenschlein, S. Influence of the Gut Microbiota Composition on Campylobacter jejuni Colonization in Chickens. Infect Immun 2017, 85, e00380, doi: 10.1128/iai.00380-17
5. Oakley, B.B.; Kogut, M.H. Spatial and Temporal Changes in the Broiler Chicken Cecal and Fecal Microbiomes and Correlations of Bacterial Taxa with Cytokine Gene Expression. Front Vet Sci 2016, 3, 11, doi: 10.3389/fvets.2016.00011
6. Gu, L.; Jiang, Q.; Chen, Y.; Zheng, X.; Zhou, H.; Xu, T. Transcriptome-wide study revealed m6A and miRNA regulation of embryonic breast muscle development in Wenchang chickens. Front Vet Sci 2022, 9, 934728, doi: 10.3389/fvets.2022.934728
7. Monk, J.M.; Turk, H.F.; Fan, Y.Y.; Callaway, E.; Weeks, B.; Yang, P.; McMurray, D.N.; Chapkin, R.S. Antagonizing arachidonic acid-derived eicosanoids reduces inflammatory Th17 and Th1 cell-mediated inflammation and colitis severity. Mediators Inflamm 2014, 2014, 917149, doi: 10.1155/2014/917149
8. Monk, J.M.; Hou, T.Y.; Turk, H.F.; Weeks, B.; Wu, C.; McMurray, D.N.; Chapkin, R.S. Dietary n-3 polyunsaturated fatty acids (PUFA) decrease obesity-associated Th17 cell-mediated inflammation during colitis. PLoS One 2012, 7, e49739, doi: 10.1371/journal.pone.0049739
9. Isse, F.A.; El-Sherbeni, A.A.; El-Kadi, A.O.S. The multifaceted role of cytochrome P450-Derived arachidonic acid metabolites in diabetes and diabetic cardiomyopathy. Drug Metab Rev 2022, 54, 141-160, doi: 10.1080/03602532.2022.2051045
10. Resta-Lenert, S.; Barrett, K.E. Enteroinvasive bacteria alter barrier and transport properties of human intestinal epithelium: role of iNOS and COX-2. Gastroenterology 2002, 122, 1070-1087, doi: 10.1053/gast.2002.32372
11. Eckmann, L.; Stenson, W.F.; Savidge, T.C.; Lowe, D.C.; Barrett, K.E.; Fierer, J.; Smith, J.R.; Kagnoff, M.F. Role of intestinal epithelial cells in the host secretory response to infection by invasive bacteria. Bacterial entry induces epithelial prostaglandin h synthase-2 expression and prostaglandin E2 and F2alpha production. J Clin Invest 1997, 100, 296-309, doi: 10.1172/jci119535
12. Le Faouder, P.; Baillif, V.; Spreadbury, I.; Motta, J.P.; Rousset, P.; Chêne, G.; Guigné, C.; Tercé, F.; Vanner, S.; Vergnolle, N.; et al. LC-MS/MS method for rapid and concomitant quantification of pro-inflammatory and pro-resolving polyunsaturated fatty acid metabolites. J Chromatogr B Analyt Technol Biomed Life Sci 2013, 932, 123-133, doi: 10.1016/j.jchromb.2013.06.014
13. Rognes, T.; Flouri, T.; Nichols, B.; Quince, C.; Mahé, F. VSEARCH: a versatile open source tool for metagenomics. PeerJ 2016, 4, e2584, doi: 10.7717/peerj.2584
14. Callahan, B.J.; McMurdie, P.J.; Rosen, M.J.; Han, A.W.; Johnson, A.J.; Holmes, S.P. DADA2: High-resolution sample inference from Illumina amplicon data. Nat Methods 2016, 13, 581-583, doi: 10.1038/nmeth.3869
15. Pruesse, E.; Peplies, J.; Glöckner, F.O. SINA: accurate high-throughput multiple sequence alignment of ribosomal RNA genes. Bioinformatics 2012, 28, 1823-1829, doi: 10.1093/bioinformatics/bts252
16. Bolyen, E.; Rideout, J.R.; Dillon, M.R.; Bokulich, N.A.; Abnet, C.C.; Al-Ghalith, G.A.; Alexander, H.; Alm, E.J.; Arumugam, M.; Asnicar, F.; et al. Reproducible, interactive, scalable and extensible microbiome data science using QIIME 2. Nat Biotechnol 2019, 37, 852-857, doi: 10.1038/s41587-019-0209-9
17. Logue, J.B.; Stedmon, C.A.; Kellerman, A.M.; Nielsen, N.J.; Andersson, A.F.; Laudon, H.; Lindström, E.S.; Kritzberg, E.S. Experimental insights into the importance of aquatic bacterial community composition to the degradation of dissolved organic matter. Isme j 2016, 10, 533-545, doi: 10.1038/ismej.2015.131
18. Walters, W.; Hyde, E.R.; Berg-Lyons, D.; Ackermann, G.; Humphrey, G.; Parada, A.; Gilbert, J.A.; Jansson, J.K.; Caporaso, J.G.; Fuhrman, J.A.; et al. Improved Bacterial 16S rRNA Gene (V4 and V4-5) and Fungal Internal Transcribed Spacer Marker Gene Primers for Microbial Community Surveys. mSystems 2016, 1, doi: 10.1128/mSystems.00009-15
19. Takai, K.; Horikoshi, K. Rapid detection and quantification of members of the archaeal community by quantitative PCR using fluorogenic probes. Appl Environ Microbiol 2000, 66, 5066-5072, doi: 10.1128/aem.66.11.5066-5072.2000

20. Huang, N.; Wang, M.; Peng, J.; Wei, H. Role of arachidonic acid-derived eicosanoids in intestinal innate immunity. Crit Rev Food Sci Nutr 2021, 61, 2399-2410, doi: 10.1080/10408398.2020.1777932
21. Murakami, M.; Nakatani, Y.; Atsumi, G.I.; Inoue, K.; Kudo, I. Regulatory Functions of Phospholipase A2. Crit Rev Immunol 2017, 37, 127-195, doi: 10.1615/CritRevImmunol.v37.i2-6.20
22. Pang, Y.; Liu, X.; Zhao, C.; Shi, X.; Zhang, J.; Zhou, T.; Xiong, H.; Gao, X.; Zhao, X.; Yang, X.; et al. LC-MS/MS-based arachidonic acid metabolomics in acute spinal cord injury reveals the upregulation of 5-LOX and COX-2 products. Free Radic Biol Med 2022, 193, 363-372, doi: 10.1016/j.freeradbiomed.2022.10.303
23. Kawahara, K.; Hohjoh, H.; Inazumi, T.; Tsuchiya, S.; Sugimoto, Y. Prostaglandin E2-induced inflammation: Relevance of prostaglandin E receptors. Biochim Biophys Acta 2015, 1851, 414-421, doi: 10.1016/j.bbalip.2014.07.008
24. Stenson, W.F. The universe of arachidonic acid metabolites in inflammatory bowel disease: can we tell the good from the bad? Curr Opin Gastroenterol 2014, 30, 347-351, doi: 10.1097/mog.0000000000000075
25. Yokomizo, T.; Nakamura, M.; Shimizu, T. Leukotriene receptors as potential therapeutic targets. J Clin Invest 2018, 128, 2691-2701, doi: 10.1172/jci97946
26. Nagatake, T.; Kunisawa, J. Emerging roles of metabolites of ω3 and ω6 essential fatty acids in the control of intestinal inflammation. Int Immunol 2019, 31, 569-577, doi: 10.1093/intimm/dxy086
27. Aoki, T.; Narumiya, S. Prostaglandin E(2)-EP2 signaling as a node of chronic inflammation in the colon tumor microenvironment. Inflamm Regen 2017, 37, 4, doi: 10.1186/s41232-017-0036-7
28. Morimoto, K.; Shirata, N.; Taketomi, Y.; Tsuchiya, S.; Segi-Nishida, E.; Inazumi, T.; Kabashima, K.; Tanaka, S.; Murakami, M.; Narumiya, S.; et al. Prostaglandin E2-EP3 signaling induces inflammatory swelling by mast cell activation. J Immunol 2014, 192, 1130-1137, doi: 10.4049/jimmunol.1300290
29. Lauritsen, K.; Laursen, L.S.; Bukhave, K.; Rask-Madsen, J. In vivo effects of orally administered prednisolone on prostaglandin and leucotriene production in ulcerative colitis. Gut 1987, 28, 1095-1099, doi: 10.1136/gut.28.9.1095
30. Iikura, M.; Suzukawa, M.; Yamaguchi, M.; Sekiya, T.; Komiya, A.; Yoshimura-Uchiyama, C.; Nagase, H.; Matsushima, K.; Yamamoto, K.; Hirai, K. 5-Lipoxygenase products regulate basophil functions: 5-Oxo-ETE elicits migration, and leukotriene B(4) induces degranulation. J Allergy Clin Immunol 2005, 116, 578-585, doi: 10.1016/j.jaci.2005.04.029
31. Wang, A.; Wan, X.; Zhuang, P.; Jia, W.; Ao, Y.; Liu, X.; Tian, Y.; Zhu, L.; Huang, Y.; Yao, J.; et al. High fried food consumption impacts anxiety and depression due to lipid metabolism disturbance and neuroinflammation. Proc Natl Acad Sci U S A 2023, 120, e2221097120, doi: 10.1073/pnas.2221097120
32. Das, U.N. Essential Fatty Acids and Their Metabolites in the Pathobiology of Inflammation and Its Resolution. Biomolecules 2021, 11, 1873, doi: 10.3390/biom11121873
33. Snyder, N.W.; Golin-Bisello, F.; Gao, Y.; Blair, I.A.; Freeman, B.A.; Wendell, S.G. 15-Oxoeicosatetraenoic acid is a 15-hydroxyprostaglandin dehydrogenase-derived electrophilic mediator of inflammatory signaling pathways. Chem Biol Interact 2015, 234, 144-153, doi: 10.1016/j.cbi.2014.10.029
34. Node, K.; Huo, Y.; Ruan, X.; Yang, B.; Spiecker, M.; Ley, K.; Zeldin, D.C.; Liao, J.K. Anti-inflammatory properties of cytochrome P450 epoxygenase-derived eicosanoids. Science 1999, 285, 1276-1279, doi: 10.1126/science.285.5431.1276
35. Luo, X.Q.; Duan, J.X.; Yang, H.H.; Zhang, C.Y.; Sun, C.C.; Guan, X.X.; Xiong, J.B.; Zu, C.; Tao, J.H.; Zhou, Y.; et al. Epoxyeicosatrienoic acids inhibit the activation of NLRP3 inflammasome in murine macrophages. J Cell Physiol 2020, 235, 9910-9921, doi: 10.1002/jcp.29806
36. Li, X.J.; Suo, P.; Wang, Y.N.; Zou, L.; Nie, X.L.; Zhao, Y.Y.; Miao, H. Arachidonic acid metabolism as a therapeutic target in AKI-to-CKD transition. Front Pharmacol 2024, 15, 1365802, doi: 10.3389/fphar.2024.1365802
37. Zhou, Y.; Liu, T.; Duan, J.X.; Li, P.; Sun, G.Y.; Liu, Y.P.; Zhang, J.; Dong, L.; Lee, K.S.S.; Hammock, B.D.; et al. Soluble Epoxide Hydrolase Inhibitor Attenuates Lipopolysaccharide-Induced Acute Lung Injury and Improves Survival in Mice. Shock 2017, 47, 638-645, doi: 10.1097/shk.0000000000000767
38. Mon, K.K.Z.; Zhu, Y.; Chanthavixay, G.; Kern, C.; Zhou, H. Integrative analysis of gut microbiome and metabolites revealed novel mechanisms of intestinal Salmonella carriage in chicken. Sci Rep 2020, 10, 4809, doi: 10.1038/s41598-020-60892-9
39. Videlock, E.J.; Cremonini, F. Meta-analysis: probiotics in antibiotic-associated diarrhoea. Aliment Pharmacol Ther 2012, 35, 1355-1369, doi: 10.1111/j.1365-2036.2012.05104.x

40. Lewis, E.D.; Antony, J.M.; Crowley, D.C.; Piano, A.; Bhardwaj, R.; Tompkins, T.A.; Evans, M. Efficacy of Lactobacillus paracasei HA-196 and Bifidobacterium longum R0175 in Alleviating Symptoms of Irritable Bowel Syndrome (IBS): A Randomized, Placebo-Controlled Study. Nutrients 2020, 12, 1159, doi: 10.3390/nu12041159
41. Bahmani, S.; Azarpira, N.; Moazamian, E. Anti-colon cancer activity of Bifidobacterium metabolites on colon cancer cell line SW742. Turk J Gastroenterol 2019, 30, 835-842, doi: 10.5152/tjg.2019.18451
42. Ishikawa, H.; Matsumoto, S.; Ohashi, Y.; Imaoka, A.; Setoyama, H.; Umesaki, Y.; Tanaka, R.; Otani, T. Beneficial effects of probiotic bifidobacterium and galacto-oligosaccharide in patients with ulcerative colitis: a randomized controlled study. Digestion 2011, 84, 128-133, doi: 10.1159/000322977
43. Luo, J.; Li, Y.; Xie, J.; Gao, L.; Liu, L.; Ou, S.; Chen, L.; Peng, X. The primary biological network of Bifidobacterium in the gut. FEMS Microbiol Lett 2018, 365, 10, doi: 10.1093/femsle/fny057
44. Goldenberg, J.Z.; Yap, C.; Lytvyn, L.; Lo, C.K.; Beardsley, J.; Mertz, D.; Johnston, B.C. Probiotics for the prevention of Clostridium difficile-associated diarrhea in adults and children. Cochrane Database Syst Rev 2017, 12, Cd006095, doi: 10.1002/14651858.CD006095.pub4
45. Ahl, D.; Liu, H.; Schreiber, O.; Roos, S.; Phillipson, M.; Holm, L. Lactobacillus reuteri increases mucus thickness and ameliorates dextran sulphate sodium-induced colitis in mice. Acta Physiol (Oxf) 2016, 217, 300-310, doi: 10.1111/apha.12695
46. Schlee, M.; Harder, J.; Köten, B.; Stange, E.F.; Wehkamp, J.; Fellermann, K. Probiotic lactobacilli and VSL#3 induce enterocyte beta-defensin 2. Clin Exp Immunol 2008, 151, 528-535, doi: 10.1111/j.1365-2249.2007.03587.x
47. Terada, T.; Nii, T.; Isobe, N.; Yoshimura, Y. Effects of Probiotics Lactobacillus reuteri and Clostridium butyricum on the Expression of Toll-like Receptors, Pro- and Anti-inflammatory Cytokines, and Antimicrobial Peptides in Broiler Chick Intestine. J Poult Sci 2020, 57, 310-318, doi: 10.2141/jpsa.0190098
48. Graßhoff, H.; Comdühr, S.; Monne, L.R.; Müller, A.; Lamprecht, P.; Riemekasten, G.; Humrich, J.Y. Low-Dose IL-2 Therapy in Autoimmune and Rheumatic Diseases. Front Immunol 2021, 12, 648408, doi: 10.3389/fimmu.2021.648408
49. Khan, S.; Moore, R.J.; Stanley, D.; Chousalkar, K.K. The Gut Microbiota of Laying Hens and Its Manipulation with Prebiotics and Probiotics To Enhance Gut Health and Food Safety. Appl Environ Microbiol 2020, 86, e00600, doi: 10.1128/aem.00600-20
50. Al-Khalaifa, H.; Al-Nasser, A.; Al-Surayee, T.; Al-Kandari, S.; Al-Enzi, N.; Al-Sharrah, T.; Ragheb, G.; Al-Qalaf, S.; Mohammed, A. Effect of dietary probiotics and prebiotics on the performance of broiler chickens. Poult. Sci 2019, 98, 4465-4479, doi: 10.3382/ps/pez282
51. Neveling, D.P.; Dicks, L.M.T. Probiotics: an Antibiotic Replacement Strategy for Healthy Broilers and Productive Rearing. Probiotics Antimicrob Proteins 2021, 13, 1-11, doi: 10.1007/s12602-020-09640-z
52. Huber-Ruano, I.; Calvo, E.; Mayneris-Perxachs, J.; Rodríguez-Peña, M.M.; Ceperuelo-Mallafré, V.; Cedó, L.; Núñez-Roa, C.; Miro-Blanch, J.; Arnoriaga-Rodríguez, M.; Balvay, A.; et al. Orally administered Odoribacter laneus improves glucose control and inflammatory profile in obese mice by depleting circulating succinate. Microbiome 2022, 10, 135, doi: 10.1186/s40168-022-01306-y
53. Hiraishi, K.; Zhao, F.; Kurahara, L.H.; Li, X.; Yamashita, T.; Hashimoto, T.; Matsuda, Y.; Sun, Z.; Zhang, H.; Hirano, K. Lactulose Modulates the Structure of Gut Microbiota and Alleviates Colitis-Associated Tumorigenesis. Nutrients 2022, 14, 649, doi: 10.3390/nu14030649